LANGMUIR

Article

pubs.acs.org/Langmuir

Surface Tension of Acid Solutions: Fluctuations beyond the Nonlinear Poisson−Boltzmann Theory

Tomer Markovich,[†] David Andelman,*[,†] and Rudi Podgornik[‡]

[†]Raymond and Beverly Sackler School of Physics and Astronomy, Tel Aviv University, Ramat Aviv, Tel Aviv 69978, Israel

[‡]Department of Theoretical Physics, J. Stefan Institute, and Department of Physics, Faculty of Mathematics and Physics University of Ljubljana, 1000 Ljubljana, Slovenia

ABSTRACT: We extend our previous study of surface tension of ionic solutions and apply it to acids (and salts) with strong ion−surface interactions, as described by a single adhesivity parameter for the ionic species interacting with the interface. We derive the appropriate nonlinear boundary condition with an *effective* surface charge due to the adsorption of ions from the bulk onto the interface. The calculation is done using the loop-expansion technique, where the zero loop (mean field) corresponds of the full nonlinear Poisson−Boltzmann equation. The surface tension is obtained analytically to one-loop order, where the mean-field contribution is a modification of the Poisson−Boltzmann surface tension and the one-loop contribution gives a generalization of the Onsager−Samaras result. Adhesivity significantly affects both contributions to the surface tension, as can be seen from the dependence of surface tension on salt concentration for strongly absorbing ions. Comparison with available experimental data on a wide range of different acids and salts allows the fitting of the adhesivity parameter. In addition, it identifies the regime(s) where the hypotheses on which the theory is based are outside their range of validity.

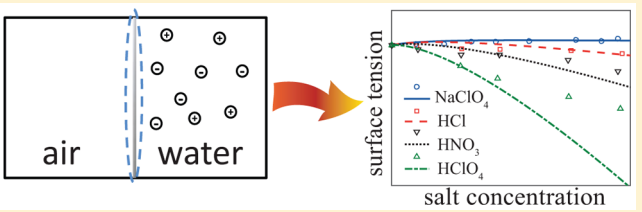

I. INTRODUCTION

Solubilization of simple salts in aqueous solutions increases, in general, its surface tension.[1,2] The theoretical foundation of this phenomenon goes back almost a century ago to Wagner,[3] who suggested an explanation based on image charges (due to the water/air dielectric discontinuity). Onsager and Samaras (OS), in their *tour de force* paper, combined this idea with the Debye−Hückel (DH)[4] theory and calculated the dependence of surface tension on salt concentration.[5] While being overall successful under low salinity conditions, the OS prediction implies the same increment of the surface tension for all monovalent salts, a finding that is at odds with many well-explored physical situations.[6] Moreover, some simple monovalent acids and bases not only show a quantitative discrepancy with the OS result but even act contrary to its qualitative features. These acids and bases may reduce the surface tension even in the low-salinity limit where the OS result is supposed to be universally valid.

A vast number of attempts that go beyond the OS theory have been proposed and incorporate ion-specific effects.[6] They are related to a much broader behavior of solutes in salt solutions observed already in the late 19th century by Hofmeister and co-workers,[7] known nowadays as the *Hofmeister series*. This series emerges in numerous chemical and biological systems,[8−10] including, but not limited to, forces between mica or silica surfaces[11−13] as well as the surface tension of electrolyte solutions.[14,15]

Over the years, different theoretical approaches were devised to incorporate these experimental findings into a generalized theoretical framework. Specifically, in order to incorporate ion-specific interactions, the well-known Poisson−Boltzmann (PB) theory was often taken as a point of departure. Such an approach, pioneered by Ninham and co-workers,[16] was later extended by Levin and co-workers.[17] The Boltzmann weight factor was modified by adding in an *ad hoc* manner different types of ion-specific interactions (assumed to be additive), such as dispersion interactions,[18−20] image-charge interaction, the Stern exclusion layer, ionic cavitation energy, and ionic polarizability.[17] Detailed explicit solvent-atomistic molecular-dynamics (MD) simulations were also invoked to derive the nonelectrostatic, ion-specific potentials of mean force in order to combine the PB equation with the ionic-specific interaction.[21,22] (See also the pertinent discussion in refs 23 and 24). Similar lines of thought were used to investigate ion density and partitioning close to interfaces[25,26] and the surface tension behavior of complicated dicarboxylic and hydroxycarboxylic acids.[27]

The above-mentioned modification of the Boltzmann weight factor was used to calculate numerically the surface tension of electrolytes at the water/air interface and with the addition of dispersion forces also at the oil/water interface.[28] Similarly, the surface tension of acids[29] was computed by taking into account the preferential adsorption of hydrogen (in the form of hydronium ions) to the interface. We note that whereas these additional interaction terms may represent real physical mechanisms underlying the specific ion−surface interactions, these terms are, in general, nonadditive.[6]

Received: August 28, 2016
Revised: November 12, 2016
Published: November 17, 2016

DOI: 10.1021/acs.langmuir.6b03186
Langmuir XXXX, XXX, XXX−XXX

In our previous works,[23,24] we introduced a self-consistent phenomenological approach that describes specific ion−surface interactions in the form of surface coupling terms in the free energy. Furthermore, on a formal level, we argued that the original OS result is, in fact, fluctuational in nature, and it is necessary to extend the PB formalism to account for fluctuations. This conceptual and formal development allowed us to derive an analytical theory that reunites the OS result with the ionic specificity of the Hofmeister series. Our results demonstrate that simple specific ion−surface interactions can explain the appearance of the Hofmeister series.

Using the one-loop expansion beyond the linearized Poisson−Boltzmann theory (the DH theory), we have developed a consistent theory[23,24] of the surface tension dependence on salinity that is in general agreement with experiment and also well reproduces the reverse Hofmeister series. Because this linearized theory is valid only for *weak* ion−surface interactions, it is not fully applicable to the case of strongly adhering ions such as some acids. It is exactly this issue that is addressed in the present work, where we use a more general approach based on a full nonlinear theory that is applicable for both *weak and strong* ion−surface interactions.

The extension to strong surface−ion interactions as parametrized by the phenomenological *adhesivity* allows us to derive the surface tension of acids and other strongly adhering ions. Our theory can successfully fit the experimentally determined surface tension in a wide range of different salts or acids with moderate adhesivity (up to a concentration of ∼1 M) and acids with high adhesivity (up to a concentration of ∼0.4 M) and is also in accord with the reverse Hofmeister series for acids. Nevertheless, in some regimes, such as high ion concentration, our calculations that incorporate ion specificity through a single phenomenological parameter (adhesivity) fail. They would have to be modified in order to take into account steric effects that are not included in the standard PB formulation. We discuss the failings of the theory and identify several possible venues of improvement.

The acids we considered in this work are assumed to be strong. This means that for a simple monovalent acid dissociated in water,

$$\mathrm{HX} \leftrightarrows \mathrm{H^+} + \mathrm{X^-} \tag{1}$$

the pK of the acid dissociation reaction is smaller than roughly −1.5. In this case, the HX acid is always fully dissociated, irrespective of all of the other parameters, and the $\mathrm{H^+}$ concentration is the same as the bulk acid concentration, $[\mathrm{H^+}] = n_b$. On the contrary, for weak acids, the amount of $\mathrm{H^+}$ is smaller than n_b and depends on n_b as well as on the acid pK. Treating weak acids is rather a simple extension of the strong acid case, addressed in this article, if one takes the pK value to be constant throughout the solution.[30]

The outline of the article is as follows. In the next section, we present our model (Section II) and calculate the mean-field electrostatic potential and the thermodynamic grand canonical potential (Section II.A), followed by the one-loop correction to the grand potential (Section II.B). Section III includes the surface tension results up to one-loop order, and in Section IV, we compare these analytical expressions with experiments. Finally, we draw our conclusions in Section V. Appendix A extends our model to include both adhesivity and fixed surface charges, and in Appendix B, we compute the surface tension for strong surface potential and negative anion adhesivity.

II. THE MODEL

The general problem we consider is the same as in our previous work,[24] composed of aqueous and air phases, as is depicted schematically in Figure 1. Because the full details can be found in section II of ref 24, only some pertinent highlights of the model are addressed.

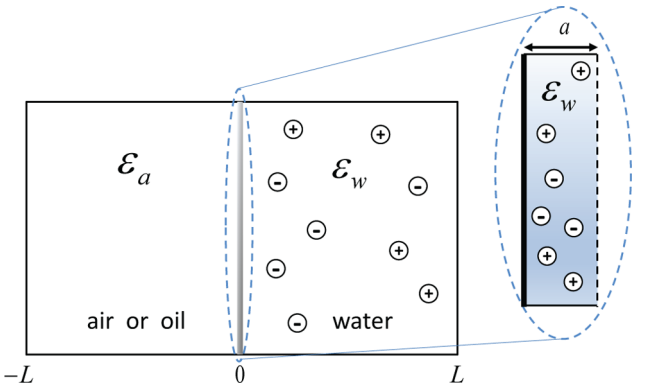

Figure 1. Schematic setup of the system. The aqueous and air phases have the same longitudinal extension, L, which is taken to be macroscopic, $L \to \infty$. A small layer proximal to the dividing surface, $0 < z < a$, exists inside the aqueous phase. Within this layer, the anions and cations interaction with the interface at $z = 0$ is modeled by a nonelectrostatic potential, $V_\pm(z)$. This potential is zero outside the proximal layer.

We consider a symmetric monovalent (1:1) electrolyte solution of bulk concentration n_b. The aqueous phase (water) volume $V = AL$ has a cross-section A and an arbitrary macroscopic length $L \to \infty$, with the dividing surface between the aqueous and the air phases at $z = 0$. The two phases are taken as two continuum media with uniform dielectric constants, ε_w and ε_a, respectively. We explicitly assume that the ions are confined in the aqueous phase because the large electrostatic self-energy penalty for placing an ion in a low dielectric medium (air or oil).

The model Hamiltonian is

$$H = \frac{1}{2}\sum_{i,j} q_i q_j u(\mathbf{r}_i, \mathbf{r}_j) - \frac{e^2}{2} N u_b + \sum_i V_\pm(z_i) \tag{2}$$

The first term is the usual Coloumbic interaction, where the summation is carried out over all of the ions in solution, $q_i = \pm e$ represents the charges of monovalent cations and anions, respectively, and N is the total number of ions in the system. The second term includes the diverging self-energy, u_b, and the last term takes into account the nonelectrostatic ion−surface potential, $V_\pm(z)$. The potential $V_\pm$ is short-ranged and confined to the proximal layer next to the dividing surface, $z \in [0, a]$. The length a is a microscopic length scale corresponding to the average ionic size or, equivalently, to the minimal distance of approach between ions. (See refs 17 and 24 for justification.)

The grand canonical partition function defined by the above Hamiltonian, eq 2, can be derived in a field theoretical form,

$$\Xi \equiv \frac{(2\pi)^{-N/2}}{\sqrt{\det[\beta^{-1}u(\mathbf{r}, \mathbf{r}')]}} \int \mathcal{D}\phi e^{-S[\phi(\mathbf{r})]} \tag{3}$$

where $\beta = 1/k_B T$ and $S[\phi(\mathbf{r})]$ plays the role of a field action,

DOI: 10.1021/acs.langmuir.6b03186
Langmuir XXXX, XXX, XXX−XXX

$$S[\phi(\mathbf{r})] = \int d\mathbf{r}\left(\frac{\beta\varepsilon(\mathbf{r})}{8\pi}[\nabla\phi(\mathbf{r})]^2 - 2\lambda\cos[\beta e\phi(\mathbf{r})]\right) - \lambda\int d^2r\int_0^a dz\Big[e^{-i\beta e\phi(\mathbf{r})}(e^{-\beta V_+(z)} - 1) + e^{i\beta e\phi(\mathbf{r})}(e^{-\beta V_-(z)} - 1)\Big] \quad (4)$$

The derivation of the above equation employs the form of the inverse Coulomb kernel $u^{-1}(\mathbf{r}, \mathbf{r}') = -\frac{1}{4\pi}\nabla\cdot[\varepsilon(\mathbf{r})\nabla\delta(\mathbf{r} - \mathbf{r}')]$ and the electroneutrality condition that requires $\lambda_+ = \lambda_- \equiv \lambda$. The fugacities are defined via the chemical potentials $\mu_\pm$, where the ion bulk self-energy, u_b, is included in their definition,

$$\lambda_\pm = a^{-3}\exp(\beta\mu_\pm)\exp\left(\frac{\varepsilon_w}{2}l_B u_b\right) \quad (5)$$

with $l_B = e^2/\varepsilon_w k_B T$ being the Bjerrum length. The grand potential, $\Omega = -k_B T \ln \Xi$, can be written to first order in a systematic loop expansion, yielding

$$\beta\Omega \simeq \beta\Omega_{MF} + \beta\Omega_{1L} = S[\psi] + \frac{1}{2}\mathrm{Tr}\ln H_2(\mathbf{r}, \mathbf{r}') \quad (6)$$

where the mean-field (MF) term, Ω_{MF}, that depends on the MF electrostatic potential, $\psi(\mathbf{r})$, is derived from the saddle-point equation

$$\left.\frac{\delta S[\phi(\mathbf{r})]}{\delta\phi(\mathbf{r})}\right|_{\phi=i\psi} = 0 \quad (7)$$

and the Hessian, related to Ω_{1L}, is defined as

$$H_2(\mathbf{r}, \mathbf{r}') = \left.\frac{\delta^2 S}{\delta\phi(\mathbf{r})\,\delta\phi(\mathbf{r}')}\right|_{\phi=i\psi} \quad (8)$$

Assuming that the ion−surface nonelectrostatic potential (Figure 1) is shorter-ranged than any other interaction, we can take the $a \to 0$ limit in the continuum theory. Then, the field action S can be decomposed into separate volume (V) and surface (S) terms

$$S[\phi(\mathbf{r})] = \int_V d\mathbf{r}\left(\frac{\beta\varepsilon(\mathbf{r})}{8\pi}[\nabla\phi(\mathbf{r})]^2 - 2\lambda\cos[\beta e\phi(\mathbf{r})]\right) - \int_S d^2r\,\lambda_s\left(\chi_+ e^{-i\beta e\phi(z=0)} + \chi_- e^{i\beta e\phi(z=0)}\right) \quad (9)$$

where we introduced a phenomenological surface interaction strength, $\chi_\pm$, in order to describe the specific short-range interaction between ions and the surface. The $\chi_\pm$ parameter is explicitly connected to another surface interaction parameter, $\alpha_\pm$, by

$$\chi_\pm \equiv a(e^{-\beta\alpha_\pm} - 1) \quad (10)$$

where $\alpha_\pm$, also known as *adhesivity*, is related to the average of the microscopic surface potential,

$$e^{-\beta\alpha_\pm} = a^{-1}\int_0^a dz\, e^{-\beta V_\pm(z)} \quad (11)$$

We note that the above decomposition into bulk and surface terms enforces the partitioning of ions into bulk and surface-residing. Thus, one also needs to introduce a specific surface fugacity, λ_s, that is different from the bulk one, $\lambda_s = \lambda\exp[\varepsilon_w l_B(u_s - u_b)/2]$. This surface fugacity includes the ion self-energy at the surface, $u_s \neq u_b$, as elaborated on in section II.B of ref 31.

The ion−surface properties as introduced above are completely codified by the $\chi_\pm$ parameter (eq 10). In the case of either repulsive or small attractive ion−surface interactions, $\chi_\pm$ is small, and only terms of order $O(\chi_\pm)$ need to be considered. This limit consistently leads to an effective Debye−Hückel (DH) theory as was elaborated on in great detail in refs 23 and 24. However, for strong ion−surface interactions, $\chi_\pm$ can be finite, and one should generally keep all orders of $\chi_\pm$. This further implies that the electrostatic potential cannot be linearized. Rather, one needs to employ the full nonlinear PB theory.

The one-loop grand potential (eq 6) is the starting point for our calculation. It constitutes a mean-field term and a fluctuation term. The mean-field term, Ω_{MF}, is derived by substituting the field action (eq 9) into eq 6,

$$\Omega_{MF} = k_B T S[\psi] = -\int d\mathbf{r}\frac{\varepsilon(\mathbf{r})}{8\pi}[\nabla\psi]^2 - 2n_b k_B T\int d\mathbf{r}\cosh(\beta e\psi) - n_b k_B T\int d^2r\left[\chi_+ e^{-\beta e\psi_s} + \chi_- e^{\beta e\psi_s}\right] \quad (12)$$

with the surface potential $\psi_s \equiv \psi(z = 0)$. The MF solution for ψ is obtained from the saddle point of the bulk part of the field action. It leads to the standard PB equation, as is shown next. The fluctuation term, Ω_{1L}, can be calculated by several routes.[32] One method is based on the use of the *argument principle*, and a second one is based on the generalized Pauli−van Vleck approach that calculates the functional integral of a general harmonic kernel. We shall proceed by employing the former methodology.[24]

II.A. Mean Field. The MF equation is derived from the saddle-point of the bulk field action. In planar geometry (Figure 1), this leads to the standard PB equation for $\psi(z)$

$$\psi''(z) = 0 \qquad z < 0,$$
$$\psi''(z) = \frac{8\pi e n_b}{\varepsilon_w}\sinh(\beta e\psi) \qquad z > 0 \quad (13)$$

where $\psi' = d\psi/dz$, and we have used the translation symmetry in the transverse (x, y) plane. We also utilized the fact that in the MF approximation the fugacities are equal to the bulk salt concentration.[24,31]

The surface part of the saddle point then gives a nonconventional boundary condition:

$$\varepsilon_w\psi'|_{0^+} - \varepsilon_a\psi'|_{0^-} = -4\pi e n_b(\chi_+ e^{-\beta e\psi_s} - \chi_- e^{\beta e\psi_s}) \quad (14)$$

where ψ_s is the surface potential and $\psi'|_{0^\pm}$ represents its left and right first derivatives at $z \to 0$. From the above equation, we can define an *effective* surface charge density, σ_{eff}, induced by the surface potential ψ_s,

$$\sigma_{eff}(\psi_s) = e n_b(\chi_+ e^{-\beta e\psi_s} - \chi_- e^{\beta e\psi_s}) \quad (15)$$

Using the fact that ψ vanishes at $z \to \pm\infty$, we obtain the usual relations:[33]

DOI: 10.1021/acs.langmuir.6b03186
Langmuir XXXX, XXX, XXX−XXX

$$\beta e\psi_s = 2\ln\left(\frac{1+\eta}{1-\eta}\right) \qquad z<0,$$
$$\beta e\psi(z) = 2\ln\left(\frac{1+\eta e^{-\kappa_D z}}{1-\eta e^{-\kappa_D z}}\right) \qquad z\geqslant 0 \tag{16}$$

The parameter $0 \leq \eta \leq 1$ is found by substituting ψ from the above equation into the boundary condition at $z = 0$ (eq 14). In addition, we have introduced the standard inverse Debye length, $\kappa_D = \lambda_D^{-1} = \sqrt{8\pi l_B n_b}$, and assumed that $|\chi_+| > |\chi_-|$, implying a positive effective surface charge and a positive surface potential. For the opposite case of $|\chi_+| < |\chi_-|$, one has to make the substitution $\eta \to -\eta$ in eq 16.

Inserting the solution of eq 16 into the boundary condition (eq 14) yields an equation for η

$$\eta^4 + \eta^3(2\kappa_D l_{GC} - 4\Delta\chi) + 6\eta^2 - \eta(2\kappa_D l_{GC} + 4\Delta\chi) + 1 = 0 \tag{17}$$

where

$$\Delta\chi \equiv \left|\frac{\chi_+ + \chi_-}{\chi_+ - \chi_-}\right|; \qquad l_{GC} \equiv \frac{1}{2\pi l_B n_b|\chi_+ - \chi_-|} \tag{18}$$

Here, $\Delta\chi$ is a modified (dimensionless) surface interaction strength (eq 10) and l_{GC} plays a similar role as the usual Gouy–Chapman length.[33] Note that the above equation applies equally to the case $|\chi_+| < |\chi_-|$.

Keeping only linear terms in $\chi_\pm$ then leads to the regular Debye–Hückel (DH) solution. For small enough bias, $|\chi_+ - \chi_-| \to 0$, we have $\kappa_D l_{GC}, \Delta\chi \gg 1$ yielding $\eta \ll 1$, and one can approximate the PB equation to order $O(\eta)$ as[23]

$$\beta e\psi_s = \frac{2}{2\Delta\chi + \kappa_D l_{GC}} \qquad z<0$$
$$\psi(z) = \psi_s e^{-\kappa_D z} \qquad z\geqslant 0 \tag{19}$$

If one furthermore assumes $\Delta\chi \ll \kappa_D l_{GC}$, which corresponds to linearization in $\chi_\pm$, then the DH solution is recovered[24]

$$\beta e\psi_s = -\frac{2}{\kappa_D l_{GC}} \tag{20}$$

When $\chi_- + \chi_+ > 0$ but either $\chi_- < 0$ or $\chi_+ < 0$, the electrostatic potential might be large and further considerations are required. We assume, without loss of generality, $|\chi_+| > |\chi_-|$ such that the effective surface charge is positive and $\chi_- < 0$. Because $\chi_- < 0$, one should keep only terms to order $O(\chi_-)$.

In Appendix B, we give further details on the complex expansion to first order in χ_- that is used for our fitting procedure (Section IV). However, in this subsection we only show the compact results obtained for $\chi_- = 0$ (zeroth order in χ_-), which is a good approximation when $|\chi_+| \gg |\chi_-|$. Taking the zeroth order in χ_- yields $\Delta\chi \to 1$, $l_{GC} \to 1/(2\pi l_B n_b \chi_+)$, and eq 17 for η takes a simpler form,

$$\eta^3 + \eta^2(2\kappa_D l_{GC} - 3) + \eta(2\kappa_D l_{GC} + 3) - 1 = 0 \tag{21}$$

The electrostatic potential, $\psi(z)$, is then derived by substituting η of eq 21 into eq 16. Hereafter, we focus on the case with $\chi_\pm > 0$, which is equivalent to $\alpha_\pm < 0$, meaning that both ions are attracted to the surface.

II.B. One-Loop Correction. In this section, we follow the one-loop calculation described in ref 24 and will not dwell much on its details. As discussed above, the one-loop correction to the grand partition function, Ω_{1L}, can be rewritten with the help of the argument principle,[32,34] converting the discrete sum of the eigenvalues of the Hessian into the logarithm of the *secular determinant* $D(k)$

$$\Omega_{1L} = \frac{1}{2}\frac{k_B T}{2}\mathrm{Tr}\ln(H_2(\mathbf{r},\mathbf{r}')) = \frac{Ak_B T}{8\pi^2}\int d^2k \ln\left(\frac{D(k)}{D_{free}(k)}\right) \tag{22}$$

where the integrand depends on the ratio $D(k)/D_{free}(k)$ and D_{free} is the reference secular determinant for a free system without ions. The secular determinant is defined as[35]

$$D = \det[M + N\Gamma(L)\Gamma^{-1}(0)] \tag{23}$$

with the matrix $\Gamma(z)$:

$$\Gamma(z) = \begin{pmatrix} h & g \\ \partial_z h & \partial_z g \end{pmatrix} \tag{24}$$

The two functions, $h(z)$ and $g(z)$, are the two independent solutions of the Hessian eigenvalue equation for zero eigenvalue,

$$\left(\frac{\partial^2}{\partial z^2} - k^2 - \kappa_D^2\cosh[\beta e\psi(z)]\right)u(z) = 0 \tag{25}$$

The corresponding boundary condition of eq 25 at $z = 0$ is

$$\varepsilon_w\partial_z u(z=0^+) - \varepsilon_a\partial_z u(z=0^-) = \omega u(0) \tag{26}$$

where we define

$$\omega \equiv \frac{1}{2}\varepsilon_w\kappa_D^2(\chi_+ e^{-\beta e\psi_s} + \chi_- e^{\beta e\psi_s}) \tag{27}$$

Matrices M and N are obtained by writing the boundary condition in a matrix form (see ref 24), yielding

$$M = \begin{pmatrix} -\omega - \varepsilon_a k & \varepsilon_w \\ 0 & 0 \end{pmatrix}; \qquad N = \begin{pmatrix} 0 & 0 \\ 0 & 1 \end{pmatrix} \tag{28}$$

Using the expression of the MF potential, $\cosh(\beta e\psi_s) = 2\coth^2[\kappa_D(z+\zeta)] - 1$ with $\zeta \equiv -(\ln\eta)/\kappa_D$, the two independent solutions of eq 25 can be written as[36]

$$h(z) = e^{pz}\left(1 - \frac{\kappa_D\coth[\kappa_D(z+\zeta)]}{p}\right)$$
$$g(z) = e^{-pz}\left(1 + \frac{\kappa_D\coth[\kappa_D(z+\zeta)]}{p}\right) \tag{29}$$

where $p^2 = k^2 + \kappa_D^2$. By substituting eq 29 into eq 23, it is straightforward to compute the secular determinant in the thermodynamical limit, $L \to \infty$. Using the limiting behaviors $g(L) \simeq g'(L) \simeq 0$, $h(L) \simeq \exp(pL)(1 - \kappa_D/p)$, and $h'(L) \simeq ph(L)$, we obtain

$$D(k) \simeq -\frac{ph(L)}{2k^2}[pg(0)(\omega + \varepsilon_a k + \varepsilon_w p) + \varepsilon_w\kappa_D^2(\coth^2(\kappa_D\zeta) - 1)] \tag{30}$$

In the DH regime, $\eta \ll 1$ and $\zeta \gg 1$. Hence, $D(k)$ reduces to

DOI: 10.1021/acs.langmuir.6b03186
Langmuir XXXX, XXX, XXX–XXX

$$D(k) \simeq -\frac{1}{2}\left[\omega + \varepsilon_a k + \varepsilon_w p\right] e^{pL} \tag{31}$$

and ω reduces to $\frac{1}{2}\varepsilon_w \kappa_D^2(\chi_+ + \chi_-)$. This is exactly the DH result, which has already been obtained in ref 23.

III. SURFACE TENSION

We can apply the formalism that was derived in the previous section to calculate the excess surface tension, $\Delta\gamma = \gamma - \gamma_{A/W}$, which is the excess ionic contribution to the surface tension with respect to the surface tension between pure water and air, $\gamma_{A/W}$. The surface tension can be calculated by using the Gibbs adsorption isotherm or, equivalently, by taking the difference between the Helmholtz free energy of an air/water system of longitudinal extent $2L$ (Figure 1) and the sum of the Helmholtz free energies of the two corresponding bulk phases (each of longitudinal extent L):

$$\Delta\gamma = \frac{F(2L) - F^{(air)}(L) - F^{(B)}(L)}{A} \tag{32}$$

The three Helmholtz free energies, $F(2L)$, $F^{(air)}(L)$, and $F^{(B)}(L)$, have yet to be calculated explicitly.

The definition of the Helmholtz free energy is

$$F = \Omega + \mu N + \mu_s N_s \tag{33}$$

where the number of ions on the surface is $N_s = -\lambda_s\, \partial\Omega/\partial\lambda_s$. Because F is independent of the fugacities,[24,37] the MF value (zeroth-loop order) of the fugacities, $\lambda = \lambda_s = n_b$, can be used.

For convenience, we separate the volume and surface contributions of the Helmholtz free energy, $F = F_V + F_A$. The volume part, F_V, is written to one-loop order[24] using eqs 5 and 33:

$$\frac{F_V}{V} \simeq \frac{\Omega_{MF}}{V} + 2k_B T n_b \ln(n_b a^3) - \frac{k_B T}{12\pi}\kappa_D^3 + \frac{k_B T}{8\pi}\kappa_D^2 \Lambda - \frac{1}{2} e^2 n_b u_b \tag{34}$$

Here, we introduced the UV cutoff $\Lambda = 2\sqrt{\pi}/a$, where a is the average minimal distance of approach between ions. This cutoff is commonly used to avoid spurious divergences arising when ions are assumed to be pointlike. (For further details, see ref 31.) In addition, we take the $\Lambda \to \infty$ limit and neglect all terms of order $O(\Lambda^{-1})$.

The first two terms in F_V are the MF grand potential (eq 12) and the usual MF entropy contribution. The third term is the well-known DH volume fluctuation term,[4] and the fourth and fifth terms are the bulk self-energies of the ions (diverging with the UV cutoff), which cancel each other exactly.

The surface part, F_A, is calculated solely from the one-loop correction

$$\frac{F_A}{A} = \frac{k_B T}{4\pi}\int_0^\Lambda dk\, k\left[\ln\left(\frac{p - \kappa_D}{k^3(\varepsilon_w + \varepsilon_a)}\right) + \ln([p + \kappa_D \coth(\kappa_D\zeta)][\omega + \varepsilon_a k + \varepsilon_w p] + \varepsilon_w \kappa_D^2(\coth^2(\kappa_D\zeta) - 1))\right] - \frac{1}{2}\frac{e^2 N_s u_s}{A} \tag{35}$$

where the last term in the above equation is proportional to the ion self-energy on the surface, u_s, which diverges with the cutoff. This last term cancels with the leading divergence of the integral at the $\Lambda \to \infty$ limit (just like the bulk one).

The bulk electrolyte free energy, $F^{(B)}$, needed for eq 32, is obtained from eqs 34 and 35 in the same way as described in Section IV of ref 24. In addition, the Helmholtz free energy of the air phase is equal to zero, $F^{(air)}(L) = 0$, because there are no ions in the air phase.

III.A. Mean Field. Using the results for the three free-energies, we calculate the surface tension to one-loop order, $\Delta\gamma \simeq \Delta\gamma_{MF} + \Delta\gamma_{1L}$. The mean-field (MF) part of the surface tension is derived using $\psi(z)$ of eqs 16 and 17,

$$\Delta\gamma_{MF} = -k_B T n_b(\chi_+ e^{-\beta e\psi_s} + \chi_- e^{\beta e\psi_s}) + \int_{-\infty}^{\infty} dz\left[-\frac{\varepsilon_w}{8\pi}\left(\frac{d\psi}{dz}\right)^2 + 2k_B T n_b(1 - \cosh\beta e\psi)\right] \tag{36}$$

In the aqueous phase $z > 0$, the first integration of eq 16 gives

$$\beta e\psi' = -2\kappa_D \sinh(\beta e\psi/2) \tag{37}$$

whereas for $z < 0$ (air), $\psi' = 0$. By inserting $\psi'(z)$ into eq 36 and integrating, we obtain the MF surface tension

$$\Delta\gamma_{MF} = -k_B T n_b[\chi_+ e^{-\beta e\psi_s} + \chi_- e^{\beta e\psi_s} + 8\kappa_D^{-1}(\cosh[\beta e\psi_s/2] - 1)] \tag{38}$$

This expression is similar to eq 3.16 of ref 38, where the surface tension was calculated for charged surfactants adsorbing onto the air/water interface. It is worth noting that by taking $\chi_\pm \to 0$ the surface potential ψ_s vanishes and consequently the entire MF contribution to the surface tension is zero. This leads back to the OS result, which is a fluctuation term.

III.B. One-Loop Correction. The one-loop correction to the surface tension takes the following form:

$$\Delta\gamma_{1L} = \frac{k_B T}{8\pi}\int_0^\Lambda dk\, k \ln\left[\frac{p - \kappa_D}{k^3(\varepsilon_w + \varepsilon_a)^2} \times (\varepsilon_w \kappa_D^2 \sinh^{-2}(\kappa_D\zeta) + [p + \kappa_D \coth(\kappa_D\zeta)][\omega + \varepsilon_a k + \varepsilon_w p])^2 \times \left(p^2 + p\kappa_D \coth(\kappa_D\zeta) + \frac{1}{2}\kappa_D^2 \sinh^{-2}(\kappa_D\zeta)\right)^{-1}\right] - \frac{k_B T}{4\pi}\frac{\omega\Lambda}{\varepsilon_w + \varepsilon_a} \tag{39}$$

Taking the limit of $\eta \ll 1$ (or $\zeta = -(\ln\eta)/\kappa_D \gg 1$) gives the linearized fluctuation contribution as obtained in refs 23 and 24

$$\frac{8\pi}{k_B T}\Delta\gamma_1 \simeq -\left(\frac{\varepsilon_w - \varepsilon_a}{\varepsilon_w + \varepsilon_a}\right)\frac{\kappa_D^2}{2}\left[\ln\left(\frac{1}{2}\kappa_D l_B\right) - \ln\left(\frac{1}{2} l_B \Lambda\right) - \frac{2\omega^2}{\kappa_D^2(\varepsilon_w^2 - \varepsilon_a^2)}\ln(\kappa_D \Lambda^{-1})\right] \tag{40}$$

where only Λ-dependent terms are shown. The first term in eq 40 is the well-known OS result[5,39,40] and it varies as $\sim\kappa_D^2 \ln(\kappa_D l_B)$. The second term is a correction due to the ion minimal distance of approach, with the UV cutoff being $\Lambda = 2\sqrt{\pi}/a$, and the third term is a correction related to the

DOI: 10.1021/acs.langmuir.6b03186
Langmuir XXXX, XXX, XXX−XXX

adhesivity parameters through $\omega(\alpha_\pm)$ (eq 27). For $\beta\alpha_\pm \ll 1$, the third term is negligible, and as expected, the derived surface tension agrees well with the OS result.

Finally, we note that the surface tension $\Delta\gamma$ contains the dependence on the phenomenological adhesivity parameter at the mean-field level as well as at the one-loop fluctuation level. This offers a desired generalization of the Onsager−Samaras limit but also introduces severe constraints on this parameter when used to fit the experimental data. This point is quite essential because it shows that even the phenomenological treatment of ion adsorption via adhesivity enters the theory at multiple, interconnected levels. The mean field terms *together* with the fluctuation corrections are needed in order to describe the data consistently and clearly delineate our theory from plain fitting routines or plain phenomenological ansatz.

IV. COMPARISON WITH EXPERIMENTS

We compare the numerical results for the surface tension (computed from the one-loop fluctuation correction of the MF results), $\Delta\gamma = \Delta\gamma_{MF} + \Delta\gamma_{1L}$, with experimental data. For the case where $\chi_\pm > 0$, we use eq 38 for $\Delta\gamma_{MF}$ and eq 39 for $\Delta\gamma_{1L}$. On the other hand, if either χ_+ or χ_- is negative, we expand to first order in the negative χ, as shown in Appendix B and explained in the paragraph after eq 11. Then, the MF term, $\Delta\gamma_{MF}$, is derived from eq B3, and $\Delta\gamma_{1L}$ is obtained from eqs B6−B8. For simplicity, we take the range of the ion-specific surface potential to be equal to a, the average minimal distance between cations and anions in water, yielding $a = r_+^{hyd} + r_-^{hyd}$, with the hydrated radii taken from the literature.[41,42]

Our fitting procedure is centered on obtaining the best-fitted values for the phenomenological adhesivities, $\alpha_\pm$. These adhesivities are extracted from one of the fits and uniquely determine the adhesivity value of the specific ion/interface system for the other fits. This procedure allows us to make predictions for other salt solutions. Note that the surface tension is symmetric with respect to exchanging the role of cations and anions. This means that the two-parameter fit with $\alpha_\pm$ will always give two equivalent results, $\alpha_+ \leftrightarrow \alpha_-$. An alternative fitting procedure was used in ref 24 for a different case in which both adhesivities are small, $|\beta\alpha_\pm| \ll 1$. Then, $\alpha^* = \alpha_- + \alpha_+$ can be introduced as a single fit parameter yielding almost equivalent results.

In Figure 2, we compare the analytical results for the surface tension of acids at the air/water interface with experimental data. The experimental data show that the surface tension decreases or slightly increases with ionic concentration. This indicates a relatively strong ion−surface interaction that cannot be treated within the DH linear theory and is consistent with our starting point. The three HX acids,[2] with X = Cl^-, NO_3^-, or ClO_4^-, and a salt with an oxy anion, $NaClO_4$,[29,43] are used in the comparison. We fit their surface tension curves with α_{Na}, α_{Cl}, and α_{NO_3}, which were derived in our previous work.[24]

In the fitting procedure, we first fit the surface tension of HCl and $NaClO_4$ in order to find α_H and α_{ClO_4}. This allows us to predict the surface tension of HNO_3 and $HClO_4$. The ionic radii for all ions except hydrogen are taken from ref 41, and the hydrogen effective radius in water is taken from ref 42. (The effective hydrogen radius includes its various complexations with water molecules.) The surface tension for $NaClO_4$ and HCl is in very good agreement with experiments for the entire concentration range (up to ∼1 M), but for HNO_3 and $HClO_4$ it shows a deviation from experiments at high concentrations (≳0.7 M for HNO_3 and ≳0.4 M for $HClO_4$).

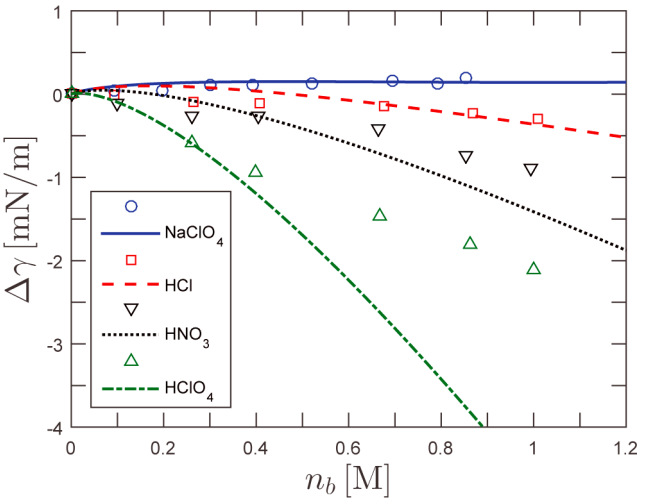

Figure 2. Comparison of the fitted surface tension, $\Delta\gamma$, with experiments as a function of salt concentration, n_b, at the air/water interface. Experimental data are taken from ref 2 for acids HCl, HNO_3, and $HClO_4$ and from refs 29 and 43 for $NaClO_4$. The adhesivity values of α_H and α_{ClO_4} are found by first fitting HCl and $NaClO_4$, while taking $\alpha_{Cl} = 0.09k_BT$ and $\alpha_{Na} = 0.11k_BT$.[24] We then use the values of α_H and α_{ClO_4} and the previously obtained $\alpha_{NO_3} = -0.05k_BT$[24] to plot our predictions for the surface tension of $HClO_4$ and HNO_3. The fitted adhesivity values are shown in Table 1. Other parameters are T = 300 K, ε_w = 80 (water), and ε_a = 1 (air).

Table 1. Fitted Values of the Phenomenological Surface Interaction Strength, $\chi_\pm$ (in Å), and the Corresponding Microscopic Adhesivity, $\alpha_\pm$ (in k_BT), at the Air/Water and Dodecane/Water Interfaces[a]

	a	χ_-	χ_+	α_-	α_+
			air/water		
HCl	4.32	−0.35	4.34	0.09	−0.70
HNO_3	4.35	0.21	4.37	−0.05	−0.70
$HClO_4$	4.38	2.43	4.40	−0.44	−0.70
$NaClO_4$	6.96	3.86	−0.73	−0.44	0.11
			oil/water		
KCl	6.63	1.7	−1.12	−0.23	0.18
KBr	6.61	3.4	−1.12	−0.41	0.18
KI	6.62	8.18	−1.12	−0.80	0.18

[a]The $\alpha_\pm$ values are obtained by the procedure elaborated in the text, including predictions for $HClO_4$ and HNO_3. The radii, a (in Å), for all ions (except H^+) are taken from ref 41. The effective H^+ radius is taken from ref 42. Note that all numerical values in the table and throughout the paper are rounded to two decimal places.

To further investigate the source of these deviations, we plot in Figure 3 three fitting curves for (a) HNO_3 and for (b) $HClO_4$. The first plot is our prediction as seen in Figure 2, the second uses α_H and then fits the best value for α_{NO_3} and α_{ClO_4}, and the third is the "best fit" optimized for both α values. Note that the two latter fits are not part of our fitting procedure and are used only to understand the deviations of the theory from experiments at high concentrations. In the first two fits, we use $\alpha_H = -0.70k_BT$ in Table 1. The second curve fits rather well, certainly better than the prediction of the first curve, and corresponds to less negative adhesivity values: $\alpha_{NO_3} = 0.01k_BT$

DOI: 10.1021/acs.langmuir.6b03186
Langmuir XXXX, XXX, XXX−XXX

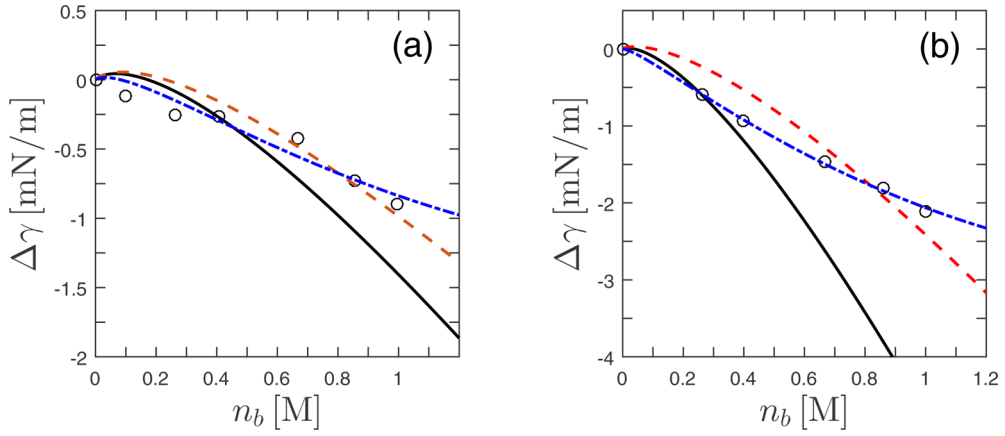

Figure 3. Comparison of the calculated surface tension (black circles) with experiments at the air/water interface as a function of ionic concentration, n_b, for HNO_3 (a) and $HClO_4$ (b). The predicted black solid line is calculated from the procedure given in the text for $\alpha_{ClO_4} = -0.44k_BT$ and $\alpha_{NO_3} = -0.05k_BT$ (Table 1). The red dashed line is a one-parameter fit for α_{ClO_4} and α_{NO_3}, yielding less negative or even positive adhesivity values: $\alpha_{ClO_4} = -0.17k_BT$ and $\alpha_{NO_3} = 0.01k_BT$. For both curves, we use $\alpha_H = -0.70k_BT$ (Table 1). The third, blue dashed−dotted line is the "best fit" (two-parameter fit) yielding $\alpha_H = -1.11k_BT$ and $\alpha_{NO_3} = 0.17k_BT$ for HNO_3, and $\alpha_H = -1.57k_BT$ and $\alpha_{ClO_4} = 0.17k_BT$ for $HClO_4$. Other parameters are the same as in Figure 2.

(as opposed to $\alpha_{NO_3} = -0.05\ k_BT$) and $\alpha_{ClO_4} = -0.17k_BT$ (as opposed to $\alpha_{ClO_4} = -0.44k_BT$). The difference in the estimated adhesivities between the first two fits implies the existence of a mechanism that will tend to diminish their values, effectively excluding the ions from the surface. A possible source of this exclusion can be associated with steric ion−ion repulsion at the surface. (This exclusion depends on ionic size and precludes unbound densities of the adsorbed ions in the limit $\beta\alpha_\pm \to -\infty$, setting an upper bound corresponding to the close-packing configuration, and is similar to systems with a charge-regulated boundary condition.[33,44])

In addition, our approach successfully applies to other types of liquid interfaces, such as oil/water. This is demonstrated in Figure 4, where we compare the calculated surface tension for the dodecane/water interface with experiments. The fits are done for three different salts having K^+ as their common cation, and they are in very good agreement with experiments. The adhesivity values are obtained by first fitting the KI data. Then, this value of $\alpha_K = 0.18k_BT$ is used in order to fit the surface tension of the two homologous salts, KBr and KCl. Notice that the adhesivity values for KCl and KBr are moderate and, thus, the fits to experiments are only slightly improved as compared to the linearized DH theory of ref 24. However, $\alpha_I \simeq -0.8k_BT$ is quite high, and the corresponding fit for KI is greatly improved when compared to that in ref 24.

Together with the previous results of ref 24, we obtain an extended reverse Hofmeister series with decreasing adhesivity strength at the air/water interface: $F^- > IO_3^- > Cl^- > BrO_3^- > Br^- > ClO_3^- > NO_3^- > I^- > ClO_4^-$. For cations, the series is $K^+ > Na^+ > H^+$. At the oil/water interface as in Figure 4, the same reversed Hofmeister series emerges with more attractive ion−surface interactions. This effect is substantially stronger for the anions and might be connected with the stronger dispersion forces at the oil/water interface[18] or a change in the strength of hydrogen bonds close to the surface. (See ref 24 for further discussion.)

V. CONCLUSIONS

Our present work complements previous results obtained for the surface tension of weakly adhering electrolytes[23,24] and extends them to strong acids, bases, and other ions that strongly adsorb to the interface. This study is accomplished by considering the full nonlinear PB theory for mean-field and one-loop fluctuation corrections, which is valid for any strength of the ion−surface interaction (the surface adhesivity parameter, α, in our model). In particular, we were able to obtain *analytically* the surface tension up to one-loop order. As was explained before, the fluctuation correction is paramount to this endeavor as it generalizes the OS argument, which is itself fluctuational in nature.[23,24]

The analytical expressions derived for the surface tension are applicable to any adhesivity values and reduce to results we derived previously for small adhesivity asymmetry ($\alpha_+ \simeq \alpha_-$). Nevertheless, we expect that for the extreme case of strong adhesivities and high salt concentration, other effects such as ion−ion steric interactions will play a role. Our results for the surface tension are in accord with the reverse Hofmeister series at the oil/water interface and extend the series to acids.

It is possible to generalize our model to include the surface tension of weak acids. Conceptually, the main change will be that the molarity of H^+ is a function of the bulk concentration, n_b, and the pK, $[H^+] = f(n_b, pK)$. As written in the Introduction, this task is rather simple if one takes the pK value to be constant throughout the solution.[30] However, the corresponding equations that take fully into account the *local* acid dissociation reaction are more complex, though imminently solvable (ref 46). Such a relation will be needed in order to compute the surface tension as a function of the experimental controlled molarity of the acid solution, n_b.

Furthermore, as already alluded to in the discussion pertaining to Figure 3, our theory consistently overestimates the surface tension at larger salt concentrations. A possible generalization that would address this issue is to incorporate steric effects either between the ions in the vicinal solution and/or between the ions already adsorbed onto the surface. This should follow the general lines elaborated in refs 47 and 48 with

DOI: 10.1021/acs.langmuir.6b03186
Langmuir XXXX, XXX, XXX−XXX

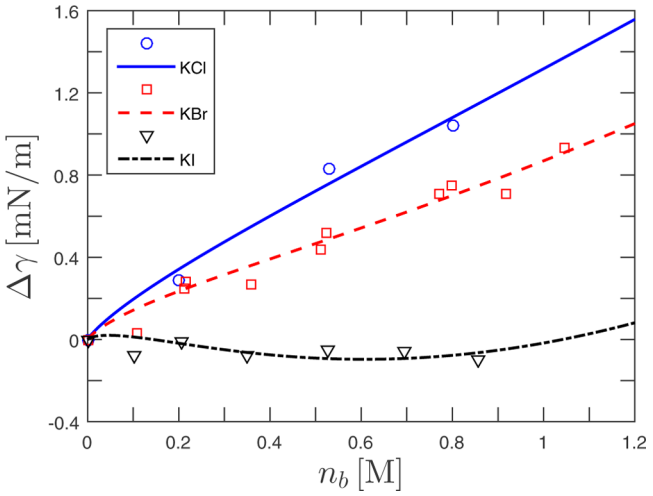

Figure 4. Comparison of the calculated surface tension with experimental data from ref 45 as a function of ionic concentration, n_b, at the dodecane/water interface. The three halide/alkaline salts are KCl, KBr, and KI. The adhesivities values are extracted from first fitting the KI curve. Then, we use the value of $\alpha_K = 0.15 k_B T$ and fit the surface tension of the other two salts, KBr and KCl. The fitted adhesivity values, $\alpha_\pm$, are shown in Table 1. Other parameters are the same as in Figure 2, beside the dielectric constant of dodecane, $\varepsilon_a = 2$.

the main consequence of diminishing the crowding of the ions next to the surface, thus effectively preventing their nonphysical accumulation leading to an overestimate in the calculated surface tension. This effect would be furthermore enhanced when steric exclusion right at the surface itself, and not only in the vicinal solution, is taken into account, resulting in further regulation of the effective surface charge along the lines of ref 44. All of these generalizations, while formally feasible, would introduce additional "fine structure" into our theory. While enhancing the theory realism when confronted with experiments, it would also preclude a simple identification of the salient mechanisms responsible for the observed behavior of the surface tension.

Finally, we note that ion−surface interactions are the core of the ionic-specific Hofmeister series. This statement is based on the generality of our model, its natural inclusion of the OS result, and the very good fit to experimental data. With the same simple idea and by merely taking into account the ion−surface specific interactions, we were able to recover the reverse Hofmeister series and calculate the surface tension for weakly adsorbed ions at a surface[23] or within a proximal layer,[24] strongly adsorbed ions or acids (the present work), and ionic profiles in the vicinity of the interface.[31]

Although our theory cannot initially predict the value of the adhesivity parameter, it can describe all of the ion-specific effects at the interface in terms of this parameter and give predictions based on previous fittings. Thus, it clearly identifies it as the main factor in determining the variation of the surface tension with ionic type, providing a consistent description of the experimentally observed functional dependence of the surface tension. In addition, it also provides mechanistic and microscopic insight into the nature of the phenomenological parameters that can, in principle, be calculated from a microscopic ion−surface interaction potential and has full predictive power in the range of small to medium ion concentrations (up to ∼0.4 M) for the more adhesive acids and for higher concentrations (up to ∼1 M) for less adhesive ions. In the future, we hope that a better understanding of the behavior of ions at interfaces will rely on more refined models that will explore the microscopic origin of the adhesivity parameter, α.

APPENDIX A: ADDING EXTERNAL SURFACE CHARGE

Throughout this work, we considered surfaces that are characterized by an adhesivity parameter, α, that is responsible for the ionic profiles in the surface/interface vicinity. Here, we extend these results and include fixed charge groups of density σ on the surface. Including σ with the surface adhesivity, α_+, modifies eq 9 into the form

$$S = \int_V d\mathbf{r}\left(\frac{\beta\varepsilon_w}{8\pi}[\nabla\phi(\mathbf{r})]^2 - 2\lambda\cos[\beta e\phi(\mathbf{r})]\right) - \int d\mathbf{r}[\lambda_s\chi_+ e^{-i\beta e\phi(\mathbf{r})} - i\beta\sigma\phi(\mathbf{r})]\delta(z) \quad \text{(A1)}$$

For simplicity, we consider only the cation adhesivity ($\chi_- = 0$) and assume positive adsorption for the cations such that $\chi_+ > 0$.

The MF equation (eq 13) does not change, but the boundary condition at $z = 0$ is modified

$$\varepsilon_w\psi_2'|_{0^+} - \varepsilon_a\psi_1'|_{0^-} = -4\pi(\sigma + \sigma_0 e^{-\beta e\psi_s}) \quad \text{(A2)}$$

$\psi_2'|_{0^+}$with $\sigma_0 = en_b\chi_+$. The MF solution (eq 16) depends on η, which by itself is derived from the boundary condition, eq A2,

$$\eta^3 + \eta^2(2\kappa_D l_\sigma - \Delta\sigma) + \eta(2\kappa_D l_\sigma + \Delta\sigma) - 1 = 0 \quad \text{(A3)}$$

In the above equation, we define $\Delta\sigma \equiv (3\sigma_0 - \sigma)/(\sigma_0 + \sigma)$ and $l_\sigma \equiv e/(2\pi l_B|\sigma_0 + \sigma|)$, where the latter plays the role of the Gouy−Chapman length. This is the solution for $\sigma_0 + \sigma > 0$, whereas for $\sigma_0 + \sigma < 0$, one has to take $\eta \to -\eta$ and $l_\sigma \to -l_\sigma$.

By taking $\sigma = 0$, we recover the case of no fixed surface charges (eq 16) for $\chi_- = 0$. On the other hand, if we take $\chi_+ = 0$, one obtains the well-known equation for η for a single charged surface in contact with an electrolyte:[33]

$$\eta^2 + 2\kappa_D l_\sigma\eta - 1 = 0 \quad \text{(A4)}$$

When $|\sigma_2 + \sigma| \ll 1$, it can be shown that $\eta \ll 1$. Taking only terms of order $O(\eta)$ yields

$$\beta e\psi_s \simeq \frac{2}{\kappa_D l_\sigma + \frac{\Delta\sigma}{2}} \quad z < 0, \qquad \psi = \psi_s e^{-\kappa_D z} \quad z \geqslant 0 \quad \text{(A5)}$$

If both σ and σ_0 are small, then $\kappa_D l_\sigma \gg \Delta\sigma$ and we recover the DH solution for an effective surface charge:

$$\beta e\psi_s \simeq -\frac{2}{\kappa_D l_\sigma} \quad \text{(A6)}$$

The free energies of the bulk and air phases do not change, and the MF surface tension can be derived as before:

$$\Delta\gamma_{MF} = -k_B T[n_b\chi_+ e^{-\beta e\psi_s} - \beta\sigma\psi_s + 8n_b\kappa_D^{-1}(\cosh[\beta e\psi_s/2] - 1)] \quad \text{(A7)}$$

The addition of fixed surface charge affects the one-loop correction only via the MF potential. The one-loop surface tension, $\Delta\gamma_{1L}$, can be derived from eq 39 by taking the MF potential obtained from eqs 16 and A3.

DOI: 10.1021/acs.langmuir.6b03186
Langmuir XXXX, XXX, XXX−XXX

It is clear that the addition of fixed surface charges affects only the MF surface tension, hence it can be easily incorporated into our methodology.

APPENDIX B: STRONG SURFACE POTENTIAL WITH $\chi_- < 0$

In this appendix, we compute the surface tension for the case in which either χ_+ or χ_- is negative. In such a case, the negative χ is always on the order of a. Thus, in order to be consistent with the limit taken in eq 9, one must keep only linear terms of the negative χ.

Without a loss of generality, we assume that $|\chi_+| > |\chi_-|$, such that the effective surface charge is positive. In such a case, having a strong electric potential requires $|\chi_-/\chi_+| \ll 1$. We write $\eta = \eta_0 + (\chi_-/\chi_+)\eta_1$, which implies that $\psi = \psi_0 + (\chi_-/\chi_+)\psi_1$ and is consistent with the limit $a \to 0$ of eq 9. Using this expansion in eq 16 gives

$$\begin{aligned}
\beta e\psi_s &\simeq \beta e\left(\psi_0^{(s)} + \frac{\chi_-}{\chi_+}\psi_1^{(s)}\right) \\
&= 2\ln\left(\frac{1+\eta_0}{1-\eta_0}\right) + \frac{2}{1-\eta_0^2}\frac{\chi_-}{\chi_+}\eta_1 \qquad z < 0, \\
\beta e\psi &\simeq \beta e\left(\psi_0 + \frac{\chi_-}{\chi_+}\psi_1\right) \\
&= 2\ln\left(\frac{1+\eta_0 e^{-\kappa_D z}}{1-\eta_0 e^{-\kappa_D z}}\right) + \frac{2e^{-\kappa_D z}}{1-\eta_0^2 e^{-2\kappa_D z}}\frac{\chi_-}{\chi_+}\eta_1 \quad z \geqslant 0
\end{aligned} \tag{B1}$$

Equation 17 for η takes a simpler form by using $\Delta\chi \simeq 1 + 2\chi_-/\chi_+$ and $l_{GC} \simeq l_{GC}^{(0)}(1+\chi_-/\chi_+)$,

$$\begin{aligned}
&\eta_0^3 + \eta_0^2(2\kappa_D l_{GC}^{(0)} - 3) + \eta_0(2\kappa_D l_{GC}^{(0)} + 3) - 1 = 0 \\
&\eta_1 = \eta_0\frac{4 + \kappa_D l_{GC}^{(0)} + \eta_0^2(4 - \kappa_D l_{GC}^{(0)})}{2(\eta_0 - 1)^3 + \kappa_D l_{GC}^{(0)}(3\eta_0^2 - 1)}
\end{aligned} \tag{B2}$$

where $l_{GC}^{(0)} \equiv 1/(2\pi l_B \chi_+)$.

Substituting the MF potential of eq B1, we write the MF surface tension (eq 38) to first order in χ_-/χ_+ as

$$\begin{aligned}
\Delta\gamma_{MF} = -k_B T n_b[&\chi_+ e^{-\beta e\psi_0^{(s)}} + 8\kappa_D^{-1}(\cosh[\beta e\psi_0^{(s)}/2] - 1) \\
&+ \frac{\chi_-}{\chi_+}(\chi_+[e^{\beta e\psi_0^{(s)}} - \beta e\psi_1^{(s)} e^{-\beta e\psi_0^{(s)}}] \\
&+ 4\kappa_D^{-1}\beta e\psi_1^{(s)}\sinh[\beta e\psi_0^{(s)}/2])]
\end{aligned} \tag{B3}$$

In order to expand the one-loop surface tension (eq 39) to first order in χ_-/χ_+, we first write

$$\zeta \simeq \zeta_0 + \frac{\chi_-}{\chi_+}\zeta_1 = -\frac{\ln\eta_0}{\kappa_D} - \frac{\chi_-}{\chi_+}\frac{\eta_1}{\kappa_D\eta_0} \tag{B4}$$

with

$$\begin{aligned}
\omega &\simeq \omega_0 + \frac{\chi_-}{\chi_+}\omega_1 \\
&= \frac{\varepsilon_w}{2}\kappa_D^2\chi_+ e^{-\beta e\psi_0^{(s)}}\left[1 + \frac{\chi_-}{\chi_+}(e^{2\beta e\psi_0^{(s)}} - \beta e\psi_1^{(s)})\right]
\end{aligned} \tag{B5}$$

Expanding eq 39 to first order in χ_-/χ_+ and writing $\Delta\gamma_{1L} = \Delta\gamma_0^{1L} + (\chi_-/\chi_+)\Delta\gamma_1^{1L}$, we obtain

$$\begin{aligned}
\Delta\gamma_0^{1L} = \frac{k_B T}{8\pi}\int_0^\Lambda dk\, k \ln\Bigg[&\frac{p - \kappa_D}{k^3(\varepsilon_w + \varepsilon_a)^2} \times (\varepsilon_w\kappa_D^2\sinh^{-2}(\kappa_D\zeta_0) + P\omega_{kp})^2 \\
&\times\left(pP + \frac{1}{2}\kappa_D^2\sinh^{-2}(\kappa_D\zeta_0)\right)^{-1}\Bigg] - \frac{k_B T}{4\pi}\frac{\omega_0\Lambda}{\varepsilon_w + \varepsilon_a}
\end{aligned} \tag{B6}$$

where we defined for convenience two auxiliary variables

$$\begin{aligned}
\omega_{kp} &\equiv \omega_0 + \varepsilon_a k + \varepsilon_w p \\
P &= p + \kappa_D\coth(\kappa_D\zeta_0)
\end{aligned} \tag{B7}$$

and

$$\begin{aligned}
\Delta\gamma_1^{1L} = \frac{k_B T}{8\pi}\int_0^\Lambda dk k\Bigg[&\omega_1\left(4p[\kappa_D^2 + p^2 + 2\kappa_D p\coth(\kappa_D\zeta_0)] + \frac{2\kappa_D^2[2p + P]}{\sinh^2(\kappa_D\zeta_0)}\right) \\
&- \zeta_1\frac{2\kappa_D^2}{\sinh^2(\kappa_D\zeta_0)}\Bigg(\varepsilon_w p^3 + k^2(\varepsilon_a k + \omega_0) \\
&+ 3\varepsilon_w\kappa_D^2 p + 4\varepsilon_w\kappa_D p^2\coth(\kappa_D\zeta_0) + \varepsilon_w\kappa_D^2\frac{3p + \kappa_D\coth(\kappa_D\zeta_0)}{\sinh^2(\kappa_D\zeta_0)}\Bigg)\Bigg] \\
&\times(2pP^2\omega_{kp} + \kappa_D^2\sinh^{-2}(\kappa_D\zeta_0)[\omega_{kp} + 2\varepsilon_w p]P + \varepsilon_w\kappa_D^4\sinh^{-4}(\kappa_D\zeta_0))^{-1} \\
&- \frac{k_B T}{4\pi}\frac{\omega_1\Lambda}{\varepsilon_w + \varepsilon_a}
\end{aligned} \tag{B8}$$

These analytical but rather complex expressions are used in the calculation of the surface tension throughout the article for the case in which either χ_+ or χ_- is negative.

AUTHOR INFORMATION

ORCID

David Andelman: 0000-0003-3185-8475

Notes

The authors declare no competing financial interest.

ACKNOWLEDGMENTS

We thank A. Cohen, R. M. Adar, H. Orland, and H. Diamant for useful discussions and numerous suggestions. This work was supported in part by the Israel Science Foundation (ISF) under grant no. 438/12, the US-Israel Binational Science Foundation (BSF) under grant no. 2012/060, and the ISF-NSFC joint research program under grant no. 885/15. R.P. acknowledges the hospitality of Tel Aviv University during his multiple visits there.

DOI: 10.1021/acs.langmuir.6b03186
Langmuir XXXX, XXX, XXX−XXX

REFERENCES

(1) Adamson, A. W.; Gast, A. P. *Physical Chemistry of Surfaces*, 6th ed.; Wiley: New York, 1997.

(2) Weissenborn, P. K.; Pugh, R. J. Surface Tension of Aqueous Solutions of Electrolytes: Relationship with Ion Hydration, Oxygen Solubility, and Bubble Coalescence. *J. Colloid Interface Sci.* **1996**, *184*, 550−563.

(3) Wagner, C. The surface tension of dilute solutions of electrolytes. *Phys. Z.* **1924**, *25*, 474−477.

(4) Debye, P. W.; Hückel, E. The theory of electrolytes. I. Lowering of freezing point and related phenomena. *Phys. Z.* **1923**, *24*, 185−206.

(5) Onsager, L.; Samaras, N. N. T. The Surface Tension of Debye-Hückle Electrolytes. *J. Chem. Phys.* **1934**, *2*, 528−536.

(6) Kunz, W. *Specific Ion Effects*; World Scientific: Singapore, 2009.

(7) Kunz, W.; Henle, J.; Ninham, B. W. 'Zur Lehre von der Wirkung der Salze' (about the science of the effect of salts): Franz Hofmeister's historical papers. *Curr. Opin. Colloid Interface Sci.* **2004**, *9*, 19−37.

(8) Collins, K. D.; Washabaugh, M. W. The Hofmeister effect and the behaviour of water at interfaces. *Q. Rev. Biophys.* **1985**, *18*, 323−422.

(9) Manciu, M.; Ruckenstein, E. Specific ion effects via ion hydration: I. Surface tension. *Adv. Colloid Interface Sci.* **2003**, *105*, 63−101.

(10) Kunz, W. Specific ion effects in colloidal and biological systems. *Curr. Opin. Colloid Interface Sci.* **2010**, *15*, 34−39.

(11) Dishon, M.; Zohar, O.; Sivan, U. From Repulsion to Attraction and Back to Repulsion: The Effect of NaCl, KCl, and CsCl on the Force between Silica Surfaces in Aqueous Solution. *Langmuir* **2009**, *25*, 2831−2836.

(12) Morag, J.; Dishon, M.; Sivan, U. The Governing Role of Surface Hydration in Ion Specific Adsorption to Silica: An AFM-Based Account of the Hofmeister Universality and Its Reversal. *Langmuir* **2013**, *29*, 6317−6322.

(13) Pashley, R. M. DLVO and Hydration Forces between Mica Surfaces in Li^+, Na^+, K^+, and Cs^+ Electrolyte Solutions: A Correlation of Double-Layer and Hydration Forces with Surface Cation Exchange Properties. *J. Colloid Interface Sci.* **1981**, *83*, 531−546.

(14) Long, F. A.; Nutting, G. C. The Relative Surface Tension of Potassium Chloride Solutions by a Differential Bubble Pressure Method. *J. Am. Chem. Soc.* **1942**, *64*, 2476−2482.

(15) Ralston, J.; Healy, T. W. Specific Cation Effects on Water Structure at the Air-Water and Air-Octadecanol Monolayer-Water Interfaces. *J. Colloid Interface Sci.* **1973**, *42*, 629−644.

(16) Ninham, B. W.; Yaminsky, V. Ion Binding and Ion Specificity: The Hofmeister Effect and Onsager and Lifshitz Theories. *Langmuir* **1997**, *13*, 2097−2108.

(17) Levin, Y.; dos Santos, A. P.; Diehl, A. Ions at the Air-Water Interface: An End to a Hundred-Year-Old Mystery? *Phys. Rev. Lett.* **2009**, *103*, 257802.

(18) Bostrom, M.; Williams, D. R. M.; Ninham, B. W. Surface Tension of Electrolytes: Specific Ion Effects Explained by Dispersion Forces. *Langmuir* **2001**, *17*, 4475−4478.

(19) Edwards, S. A.; Williams, D. R. M. Double Layers and Interparticle Forces in Colloid Science and Biology: Analytic Results for the Effect of Ionic Dispersion Forces. *Phys. Rev. Lett.* **2004**, *92*, 248303.

(20) Lo Nostro, P.; Ninham, B. W. Hofmeister phenomena: an update on ion specificity in biology. *Chem. Rev.* **2012**, *112*, 2286−2322.

(21) Schwierz, N.; Netz, R. R. Effective Interaction between Two Ion-Adsorbing Plates: Hofmeister Series and Salting-In/Salting-Out Phase Diagrams from a Global Mean-Field Analysis. *Langmuir* **2012**, *28*, 3881−3886.

(22) Schwierz, N.; Horinek, D.; Netz, R. R. Anionic and cationic Hofmeister effects on hydrophobic and hydrophilic surfaces. *Langmuir* **2013**, *29*, 2602−2614.

(23) Markovich, T.; Andelman, D.; Podgornik, R. Surface tension of electrolyte solutions: A self-consistent theory. *EPL* **2014**, *106*, 16002.

(24) Markovich, T.; Andelman, D.; Podgornik, R. Surface tension of electrolyte interfaces: Ionic specificity within a field-theory approach. *J. Chem. Phys.* **2015**, *142*, 044702.

(25) Ghosal, S.; Brown, M. A.; Bluhm, H.; Krisch, M. J.; Salmeron, M.; Jungwirth, P.; Hemminger, J. C. Ion partitioning at the liquid/vapor interface of a multi-component alkali halide solution: A model for aqueous sea salt aerosols. *J. Phys. Chem. A* **2008**, *112*, 12378−12384.

(26) Vacha, R.; Horinek, D.; Berkowitz, M. L.; Jungwirth, P. Hydronium and hydroxide at the interface between water and hydrophobic media. *Phys. Chem. Chem. Phys.* **2008**, *10*, 4975−4980.

(27) Mahiuddin, S.; Minofar, B.; Borah, J. M.; Das, M. R.; Jungwirth, P. Propensities of oxalic, citric, succinic, and maleic acids for the aqueous solution/vapour interface: Surface tension measurements and molecular dynamics simulations. *Chem. Phys. Lett.* **2008**, *462*, 217−221.

(28) dos Santos, A. P.; Levin, Y. Ions at the water-oil interface: interfacial tension of electrolyte solutions. *Langmuir* **2012**, *28*, 1304−1308.

(29) dos Santos, A. P.; Levin, Y. Surface tensions and surface potentials of acid solutions. *J. Chem. Phys.* **2010**, *133*, 154107.

(30) Housecroft, C. E.; Sharpe, A. G. *Inorganic Chemistry*, 4th ed.; Pearson Education Limited: Harlow, U.K., 2012.

(31) Markovich, T.; Andelman, D.; Orland, H. Ionic profiles close to dielectric discontinuities: Specific ion-surface interactions. *J. Chem. Phys.* **2016**, *145*, 134704.

(32) Dean, D. S.; Horgan, R. R.; Naji, A.; Podgornik, R. One-dimensional counterion gas between charged surfaces: exact results compared with weak- and strong-coupling analyses. *J. Chem. Phys.* **2009**, *130*, 094504.

(33) Markovich, T.; Andelman, D.; Podgornik, R. *Charged Membranes: Poisson-Boltzmann Theory, DLVO Paradigm and beyond*. In *Handbook of Lipid Membranes*; Safynia, C., Raedler, J., Eds.; Taylor & Francis, 2016.

(34) Attard, P.; Mitchell, D. J.; Ninham, B. W. Beyond Poisson-Boltzmann: Images and Correlations in the Electric Double Layer. I. Counterions only. *J. Chem. Phys.* **1988**, *88*, 4987−4996.

(35) Kirsten, K.; McKanem, A. J. Functional determinants by contour integration methods. *Ann. Phys.* **2003**, *308*, 502−527.

(36) Lau, A. W. C. Fluctuation and correlation effects in a charged surface immersed in an electrolyte solution. *Phys. Rev. E* **2008**, *77*, 011502.

(37) Démery, V.; Dean, D. S.; Podgornik, R. Electrostatic interactions mediated by polarizable counterions: weak and strong coupling limits. *J. Chem. Phys.* **2012**, *137*, 174903.

(38) Diamant, H.; Andelman, D. Kinetics of surfactant adsorption at fluid-fluid interfaces. *J. Phys. Chem.* **1996**, *100*, 13732−13742.

(39) Dean, D. S.; Horgan, R. R. Field theoretic calculation of the surface tension for a model electrolyte system. *Phys. Rev. E* **2004**, *69*, 061603.

(40) Podgornik, R.; Zeks, B. Inhomogeneous Coulomb fluid: A functional integral approach. *J. Chem. Soc., Faraday Trans. 2* **1988**, *84*, 611−631.

(41) Nightingale, E. R., Jr. Phenomenological theory of ion solvation. Effective radii of hydrated ions. *J. Phys. Chem.* **1959**, *63*, 1381−1387.

(42) Marcus, Y. Volumes of aqueous hydrogen and hydroxide ions at 0 to 200 °C. *J. Chem. Phys.* **2012**, *137*, 154501.

(43) Matubayasi, N. Unpublished work.

(44) Markovich, T.; Andelman, D.; Podgornik, R. Charge regulation: A generalized boundary condition? *EPL* **2016**, *113*, 26004.

(45) Aveyard, R.; Saleem, S. M. Interfacial tensions at alkane-aqueous electrolyte interface. *J. Chem. Soc., Faraday Trans. 1* **1976**, *72*, 1609−1617.

(46) Markovich, T.; Andelman, D.; Podgornik, R. To be submitted for publication.

(47) Borukhov, I.; Andelman, D.; Orland, H. Steric Effects in Electrolytes: A Modified Poisson-Boltzmann Equation. *Phys. Rev. Lett.* **1997**, *79*, 435−438.

DOI: 10.1021/acs.langmuir.6b03186
Langmuir XXXX, XXX, XXX−XXX

(48) Maggs, A. C.; Podgornik, R. General theory of asymmetric steric interactions in electrostatic double layers. *Soft Matter* **2016**, *12*, 1219–1229.

DOI: 10.1021/acs.langmuir.6b03186
Langmuir XXXX, XXX, XXX–XXX